THE JOURNAL OF PHYSICAL CHEMISTRY A

Article

pubs.acs.org/JPCA

Mechanochemistry: The Effect of Dynamics

Hans S. Smalø,[†] Vladimir V. Rybkin,[†,‡] Wim Klopper,[‡] Trygve Helgaker,[†] and Einar Uggerud*[,†]

[†]Centre for Theoretical and Computational Chemistry, Department of Chemistry, University of Oslo, P.O. Box 1033, N-0315 Oslo, Norway

[‡]Institute of Physical Chemistry, Theoretical Chemistry Group, Karlsruhe Institute of Technology, KIT Campus South, Fritz-Haber-Weg 2, D-76131 Karlsruhe, Germany

ABSTRACT: Dynamical effects on the mechanochemistry of linear alkane chains, mimicking polyethylene, are studied by means of molecular dynamics simulations. Butane and octane are studied using density-functional theory (DFT), whereas higher homologues are studied using a simple one-dimensional model in which the molecules are represented by a linear chain of Morse potentials (LCM). The application of a fixed external force to a thermodynamically pre-equilibrated molecule leads to a preference for cleavage of the terminal C−C bonds, whereas a sudden application of the force favors bond breaking in the central part of the chain. In all cases, transition-state theory predicts higher bond-breaking rates than found from the more realistic molecular dynamics simulations. The event of bond dissociation is related to dynamic states involving symmetric vibrational modes. Such modes do in general have lower frequencies of vibration than antisymmetric modes, which explains the deviation between the statistical theory and the dynamics simulations. The good qualitative agreement between the DFT and LCM models makes the latter a useful tool to investigate the mechanochemistry of long polymer chains.

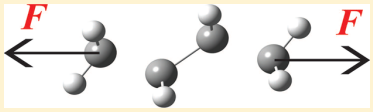

INTRODUCTION

In mechanochemistry, we study the influence of an external force on chemical properties and reactivity.[1−12] In the extreme case, an external force may induce bond dissociation within a molecule. Recently, we studied this process by quantum-chemical calculations and analyzed the results by means of a simple mechanical model.[13] It was demonstrated there and is implicit in several other works[14−16] that the mechanical strength of a bond may differ from its thermochemical strength. It was also shown that the mechanical strength of a bond depends on the harmonic force constant and the bond dissociation energy, as well as the angle of attack (the angle between the bond and the force vector).

A limitation of many studies is that the effects of dynamics are ignored in describing the bond-breaking process. Traditionally, the kinetics of mechanochemistry is analyzed using Bell's formula,[10] expressing the rate coefficient k as

$$k = \upsilon\, e^{-(E_0 - xF)/k_B T} \tag{1}$$

where υ is the frequency factor, E_0 is the critical energy without the external force, x is a distance, F is the external force, k_B is the Boltzmann constant, and T is the temperature. Bell's formula assumes that the critical energy depends linearly on the force. Often, this is a reasonable assumption; however, for bond-breaking processes, in particular, nonlinear terms must be added, leading to an extended Bell theory.[17] If the energy depends linearly on the force, then the distance x is given by the difference between the transition-state geometry and the initial-state geometry. In addition to the nonlinearity problem, we note that x is often used as an adjustable parameter when interpreting experimental results, so in any case a quantitative relationship between theory and experiment is difficult to obtain. Therefore, for a more general theoretical description, we find it more appropriate to use transition-state theory (TST) than Bell's theory, despite the simplicity of the latter. To apply TST successfully, it is important to be able to identify correctly the number of minima and the transition states of the force-modified potential-energy surface (PES), which may be different from those on the initial PES, see ref 14.

We here identify two prototypical experimental situations where mechanochemical considerations are central but, as it will turn out, in quite different ways. In the first, a polymer is anchored between the tip and the fixed base of an atomic force microscope (AFM) and then slowly stretched. In the second, the polymer is subject to forces induced in the medium by ultrasound.[18]

For simplicity, we here consider polyethylene, focusing on the breaking of C−C bonds. The strongest external force that an isolated C−C bond can withstand in the static approximation is about 6 nN. By contrast, AFM stretching experiments indicate that C−C polymer bonds typically break already at a few nN.[1] The apparent discrepancy can be understood as soon as one realizes that bond breaking is a kinetic process that is strongly temperature dependent, in accordance with kinetic theory as explained above. While polymer stretching is a slow, quasistatic process under the conditions of such AFM experiments, it is believed that force induction during ultrasound treatment is a more rapid process and that the ultrasound treatment abruptly shifts the system away from equilibrium.[2,3,18,19] In fact, direct observation shows that during ultrasound treatment bubbles are formed. When a bubble bursts, surface polymer molecules are subject to

Received: May 20, 2014
Revised: August 8, 2014
Published: August 8, 2014

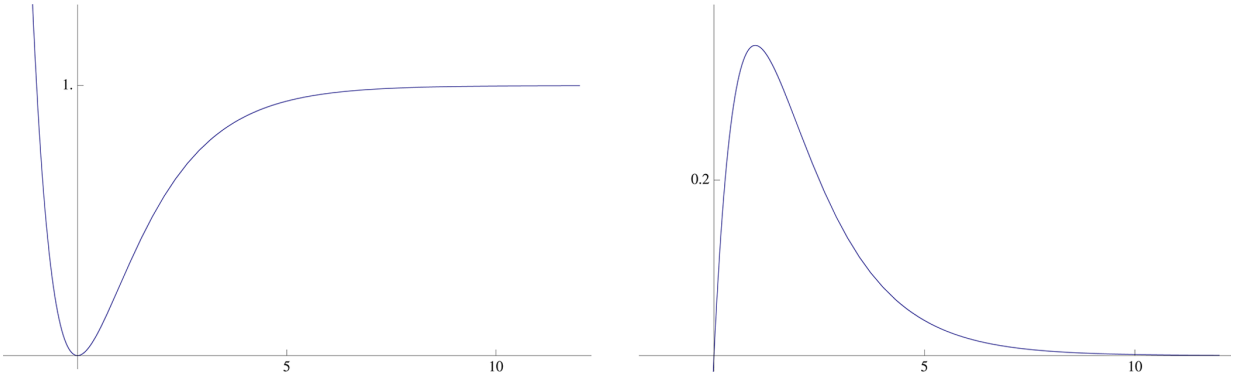

Figure 1. Morse function and its derivative.

significant mechanical impulses. Besides the important role of force induction in this process, thermal effects are important.[20]

Theoretical models describing the complex experimental situations considered above should incorporate a detailed molecular dynamics perspective. In particular, it is important to know if a statistical treatment such as TST is sufficient for predicting experimental observables (bond-breaking time as a function of the applied force, identification of the bond that breaks) or if specific dynamical effects are operative. To address these questions, we here perform a series of molecular dynamic calculations to simulate how a molecule may dissociate during the application of an external force. Our ambition is not to provide accurate theoretical treatments of the two prototypical experimental situations described above (AFM and ultrasound) but rather to identify the characteristic features of situations in which a force is applied in a controlled quasiequilibrium manner or instantly. For this purpose, it may still be useful to keep the these prototypical experimental situations in the back of our minds.

We therefore consider two scenarios, with the external force applied in the following ways.

Fixed-Force Scenario. The polymer chain is first prepared in the equilibrium configuration corresponding to an externally applied fixed force, a thermodynamically equilibrated ensemble is created, and the dynamics is run under the constraint of the fixed force. This model represents a process where the molecule is stretched gradually and kept close to thermodynamical equilibrium during the stretching.

Sudden-Force Scenario. The polymer chain is prepared in a thermodynamically equilibrated ensemble at the equilibrium geometry in the absence of an external force, and the dynamics is run following the instantaneous application of a force. Such simulations are probably most relevant for ultrasonic experiments but also serve to illustrate how large deviations from thermodynamical equilibrium may affect the system.

For each scenario, the dynamics is simulated using two different models. First, we apply classical dynamics to a simple mechanical model system, namely, a linear chain of Morse potentials (LCM). Force-field based methods have previously been used with success in this context;[14] our goal is to illustrate the difference between the dynamical and statistical-mechanics treatments. The benefits of a simple model are manifold: calculations are fast and can therefore be applied to large systems (here, up to 128 bonds and 129 atoms); it is easy to implement; the theory is transparent to mathematical analysis; and it is straightforward to control relevant parameters. Further simplifications are obtained by working with a one-dimensional system of identical atoms. We realize that the linear chain model is primitive. This artificial system was chosen for the sole purpose of having a simplest possible model of the backbone dynamics. For the purpose of a physically more realistic description of the intramolecular vibrational energy distribution (IVR) either a complete force-field model including bending and dihedral internal rotational degrees of freedom or, as will be described below, an ab initio treatment of the force field is clearly better.

Second, for a more realistic description, Born−Oppenheimer dynamics based on density-functional theory (DFT) is applied. Such a dynamics has previously been used in the context of mechanochemistry for several different systems.[21−24] Here, we use DFT to dissociate butane and octane, comparing the results with those of TST and the LCM model.

THEORY

A Simple Mechanical Model: Linear Chain of Morse Potentials. We consider a linear model system of n atoms (or more generally atom groups) on an axis with coordinates $\mathbf{r} = \{r_1, r_2, ..., r_n\}$ such that

$$r_1 < r_2 ... < r_n \tag{2}$$

There are thus $N = n - 1$ bonds in the system. We assume that the potential energy of the system is a sum of the nearest neighbor pair potentials

$$v(\mathbf{r}) = \sum_{i=2}^{n} V(r_{i,i-1}) - r_{n,1}F^{\text{ext}} \qquad r_{i,j} = r_i - r_j \tag{3}$$

and note that $r_{i,j} > 0$ when $i > j$. Each pair potential is a Morse function of the form

$$V(r) = D_e[1 - e^{-(k_e/2D_e)^{1/2}(r-R_e)}]^2 \tag{4}$$

where D_e is the bond dissociation energy, k_e is the harmonic force constant, and R_e is the equilibrium bond length. The last term in eq 3 represents the potential arising from the external force F^{ext} applied to the end groups. A positive external force $F^{\text{ext}} > 0$ stretches the molecule by favoring a larger molecular length $r_{n,1} = r_n - r_1$; conversely, a negative force $F^{\text{ext}} < 0$ compresses the molecule.

Introducing the notation

$$F_{i,j} = -F_{j,i} = -\frac{dV(r_{i,j})}{dr_i} = \frac{dV(r_{i,j})}{dr_j} \tag{5}$$

dx.doi.org/10.1021/jp504959z | J. Phys. Chem. A 2014, 118, 7683−7694

for the force acting on atom i due to atom j and noting that $F_{i,j} = 0$ unless $j = i \pm 1$, we obtain for the total force on atom i

$$F_i = -\frac{\mathrm{d}v(\mathbf{r})}{\mathrm{d}r_i} = \begin{cases} F_{1,2} - F^{\mathrm{ext}} & i = 1 \\ -F_{i-1,i} + F_{i,i+1} & 1 < i < n \\ -F_{n-1,n} + F^{\mathrm{ext}} & i = n \end{cases} \tag{6}$$

as illustrated in eq 7.

$$\overset{F^{\mathrm{ext}}}{\longleftarrow}\bullet_{i-1}\overset{F_{i-1,i}}{\longrightarrow}\quad\overset{F_{i-1,i}}{\longleftarrow}\bullet_{i}\overset{F_{i,i+1}}{\longrightarrow}\quad\overset{F_{i,i+1}}{\longleftarrow}\bullet_{i+1}\overset{F^{\mathrm{ext}}}{\longrightarrow} \tag{7}$$

At equilibrium, the total force on each atom is zero, $F_i = 0$, yielding

$$F^{\mathrm{ext}} = F_{i-1,i} = -F_{i,i-1} = \frac{\mathrm{d}V(r_{i,i-1})}{\mathrm{d}r_i} = \frac{\mathrm{d}V(r)}{\mathrm{d}r} \qquad 1 \le i \le n \tag{8}$$

In Figure 1, we have plotted the Morse function and its derivative. The maximum derivative is given by

$$F^{\mathrm{crit}} = \sqrt{\frac{D_e k_e}{8}} \tag{9}$$

The corresponding bond distance, known as the breaking-point distance, is denoted by R_{bp}. Depending on the value of the external force F^{ext} in eq 8, we have the following bond-length solutions R, see Figure 1:

1. $F^{\mathrm{ext}} < 0$: one compressed solution ($\underline{R} < R_e$)
2. $F^{\mathrm{ext}} = 0$: the equilibrium solution ($R = R_0$)
3. $0 < F^{\mathrm{ext}} < F^{\mathrm{crit}}$: two stretched solutions ($R_e < \underline{R}_{\mathrm{bp}} < R_{\mathrm{bp}} < \overline{R}_{\mathrm{bp}}$)
4. $F^{\mathrm{ext}} = F^{\mathrm{crit}}$: the breaking-point solution ($R = R_{\mathrm{bp}}$)
5. $F^{\mathrm{ext}} > F^{\mathrm{crit}}$: no solution

In short, one stable solution $R < R_{\mathrm{bp}}$ is found for all $F^{\mathrm{ext}} < F^{\mathrm{crit}}$. When $F^{\mathrm{ext}} \le 0$, there is only one stable solution of the system, with all bond distances equal to R_{cmp} (if $F^{\mathrm{ext}} < 0$) or equal to R_e (if $F^{\mathrm{ext}} = 0$). When $0 < F^{\mathrm{ext}} < F^{\mathrm{crit}}$, there are many solutions. One solution is obtained by setting all $R = \underline{R}_{\mathrm{bp}}$, while a transition-state solution is found by setting one bond distance to $\overline{R}_{\mathrm{bp}}$ and all others to R_{sub}.

Table 1. Parameters Used for the Morse Potential, Mass, and Temperature

D_e	k_e	m	T
0.18 au	0.25 au	25700 au	600 K

The Morse parameters used in this work, which are listed in Table 1, give a critical force of about 6 nN, typical of a C−C bond. A given bond length r_{ij} is calculated as

$$r_{ij}(t) = R_e + \Delta + \delta_{ij}(t) \tag{10}$$

where R_e is the equilibrium bond distance in the absence of an external force, Δ is the change in the bond length induced by the external force, and $\delta_{ij}(t)$ is the deviation from the equilibrium bond length due to thermal fluctuations.

Setting all masses to m and noting that the forces are zero unless $i = j \pm 1$, we obtain the following equations for the model dynamics by setting $j = i + 1$:

$$m_r \frac{\mathrm{d}^2\delta_{i,i+1}(t)}{\mathrm{d}t^2} = \frac{1}{2}F_{i-1,i} + \frac{1}{2}F_{j,j+1} - F_{i,j} \tag{11}$$

where m_r is the reduced mass, which is equal to $m_r = (1/2)m$ since all masses are equal. For each terminal bond, one of the forces is equal to the external force F^{ext}. We use $m = 2.57 \times 10^4 m_e$, which corresponds to the mass of a methylene group.

To compare the results of the dynamics simulations with those of TST, a transition state must be identified. In the transition state, all forces are zero and there is exactly one imaginary normal-mode frequency. Thus, the LCM transition state was found by setting all $F_{i-1,i} = F^{\mathrm{ext}}$, yielding $F_i = 0$. The bond distances are then given by eq 8, which for $0 < F^{\mathrm{ext}} < F^{\mathrm{crit}}$ has two stretched solutions for each bond: $\underline{R}_{\mathrm{bp}} < R_{\mathrm{bp}}$ and $\overline{R}_{\mathrm{bp}} > R_{\mathrm{bp}}$. The LCM equilibrium solution is found by setting all N bond distances equal to $\underline{R}_{\mathrm{bp}}$, from which a transition state is generated by replacing one (and only one) of these bond distances by $\overline{R}_{\mathrm{bp}}$, leading to N unique transition states, one for each bond. For each transition state, the critical energy E^{crit} can be calculated as

$$E^{\mathrm{crit}} = \int_{r_{ij}^{(0)}+\Delta}^{X_{\mathrm{TS}}} (F_{ij} - F^{\mathrm{ext}})\,\mathrm{d}\delta \tag{12}$$

where X_{TS} is the position of the transition state. For further technical details and discussion of the relationship between the critical energy of a static model and the bond-breaking times of dynamical models, see ref 13. In Figure 2, the critical energy E^{crit} is plotted against F^{ext} for the Morse potential with the parameters in Table 1.

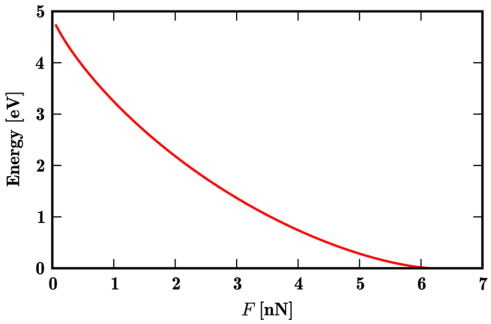

Figure 2. Critical energy as a function of external force for a Morse potential with parameters given in Table 1.

In TST, the bond-breaking rate coefficient is obtained as

$$k = v\, \mathrm{e}^{-E^{\mathrm{crit}}/k_B T} \tag{13}$$

In this expression, v is the attempt-to-escape frequency, here calculated as

$$v = \frac{k_B T}{h}\frac{Z^*}{Z} \tag{14}$$

where Z^* is the partition function of the transition state without the imaginary frequency and Z the partition function of the reactant. The average time it takes to break the bond, assuming exponential decay, is then given by

$$\tau^{\mathrm{break}} = k^{-1} \tag{15}$$

For the linear chain, Z^* is equal to the product of the vibrational partition functions of the two separate chains, whereas Z is the vibrational partition function of the entire

dx.doi.org/10.1021/jp504959z | J. Phys. Chem. A 2014, 118, 7683−7694

system. Note that, for the the LCM model, υ depends on which bond is broken. In addition, there are N distinct transition states, one for each bond, all of the same critical energy. However, applying an average value of υ in eq 14, the time it will take to break at least one bond can be written as

$$\tau^{\text{break}} = N^{-1}k^{-1} \tag{16}$$

whose logarithm is given by

$$\log \tau^{\text{break}} = -\log N - \log k = -\log N - \log \upsilon + \frac{E^{\text{crit}}}{k_{\text{B}}T} \tag{17}$$

Born−Oppenheimer Molecular Dynamics. To probe the effect of dynamics, we have performed on-the-fly Born−Oppenheimer molecular dynamics (BOMD) calculations for *n*-butane and *n*-octane with different external forces applied. All calculations were performed at the B3LYP/6-311+G** level of theory, chosen to be computationally feasible and to give results comparable with previous work.[20] Although conventional hybrid functionals fail to describe properly bond breaking without an applied external force, it has been shown that this level of theory is sufficient for the description of bond rupture by an applied external force.[25] Moreover, even though the triplet instability of restricted B3LYP theory occurs in the vicinity of the transition state with an applied external force, the difference between the restricted and unrestricted energies at the transition state is 1 kJ/mol or less (but increases with increasing fragment separation). The TST and BOMD descriptions of the first bond breaking are thus both qualitatively and quantitatively correct, while post-transition-state dynamics is probed only qualitatively.

Steered molecular dynamics[21] was applied in a simplified fashion—that is, at each time step, the force between the terminal carbon atoms was set to a constant value along the line connecting these atoms, see the potential in eq 3 and ref 26.

Transition-State Theory Calculations with DFT. For a full comparison with the LCM model, the transition states of butane and octane with an applied external force were determined at the B3LYP/6-311+G** level of theory. The rate coefficients for unimolecular dissociation were calculated using conventional TST in the harmonic approximation. The rotational degrees of freedom were disregarded, bearing in mind the restricted rotational degrees of freedom of a stretched molecule. The equilibrium and transition-state geometries are similar, indicating that the influence of rotation on the rate coefficient is small.

For the same reason, the effect of anharmonicity on the prefactors should be small. The frequencies of the most anharmonic vibrations in alkanes—namely, the torsional motion of the methyl groups—are almost identical at the equilibrium and the transition state. In fact, the only vibrational mode that contributes significantly to the rate coefficient is the vibration of the initial state along the reaction coordinate. Since this is a high-frequency chain-stretch mode, the effect of anharmonicity on the prefactor should be moderate.

Sampling. We perform the dynamics simulations in the microcanonical (NVE) ensemble. For the short-time reactive gas-phase simulations performed here, the NVE ensemble is appropriate, as collisions are rare on the time scale of the reaction, except for the longest chain in the LCM simulations. This approach makes it possible to trace intermolecular vibrational energy redistribution without external intervention. It also makes it possible to include zero-point vibrational energy, which is more important for molecular systems than for fluids. On the other hand, reaction times are short enough not to lead to significant zero-point vibrational energy leakage.

We assume that the initial conditions of the BOMD calculations can be obtained by standard ensemble methods, using the harmonic-oscillator approximation, in both the fixed-force and sudden-force cases. For the LCM model, the frequencies of vibration are obtained using the exact solution for a chain of harmonic oscillators.[27] Each normal mode is given a random energy, E_{mode}, according to the Boltzmann distribution for a classical harmonic oscillator

$$p(E_{\text{mode}}) \propto \mathrm{e}^{-E_{\text{mode}}/k_{\text{B}}T} \tag{18}$$

and a random phase. Alternatively, we can employ a quasiclassical harmonic oscillator,[28] where $\mathrm{e}^{-E_{\text{mode}}/k_{\text{B}}T}$ is rounded down to the nearest integer n and the energy of the mode of frequency ω is set to

$$E_{\text{mode}} = \left(\frac{1}{2} + n\right)\hbar\omega \tag{19}$$

Since $k_{\text{B}}T$ is typically much smaller than $\hbar\omega$, most modes are in the ground state.

Computational Details. For the LCM calculations, linear chains of 16, 32, 64, and 128 bonds were selected. For each value of the external force and chain length, we ran 96 trajectories at 300 and 600 K. We assume the validity of the harmonic approximation with oscillations around $R_0 + \Delta$ and with the harmonic force constant

$$k^{\text{eff}} = \left.\frac{\mathrm{d}^2V(r)}{\mathrm{d}r^2}\right|_{r=R_0+\Delta} \tag{20}$$

where $\Delta = 0$ in the absence of an external force.

For the DFT calculations, we have simulated microcanonical (NVE) ensembles of trajectories based on a quasiclassical normal-mode sampling[28] at 300 K without rotational sampling. For a given applied force, the normal modes were generated by diagonalizing the mass-weighted Hessian, from which not only the translational and rotational degrees of freedom but also $R = r_{n,1}$ were projected out.[29]

For each system (butane and octane), we calculated four sets of 50 trajectories using the external forces

$$F^{\text{sudden}} < F^{\text{sub}} < F^{\text{crit}} < F^{\text{super}} \tag{21}$$

with F^{sudden} applied in a sudden-force manner and the remaining forces in a fixed-force manner. The values of the forces are listed in Table 2, where F^{crit} was determined by a constrained geometry optimization.[20] In total, we report 210 trajectories for each of butane and octane.

Each trajectory was integrated for 2 ps (4000 steps) or until bond dissociation (defined to have occurred when $R \geq R_0 + 2$ Å), using the symplectic velocity-Verlet integrator[30] with time steps of 0.5 fs. The DFT calculations were performed with a development version of LSDALTON 2011 program.[31,32] For

Table 2. Applied Forces in the DFT Simulations (nN)

force	butane	octane
F^{sudden}	4.5	4.1
F^{sub}	5.2	5.3
F^{crit}	5.5	5.6
F^{super}	5.8	5.9

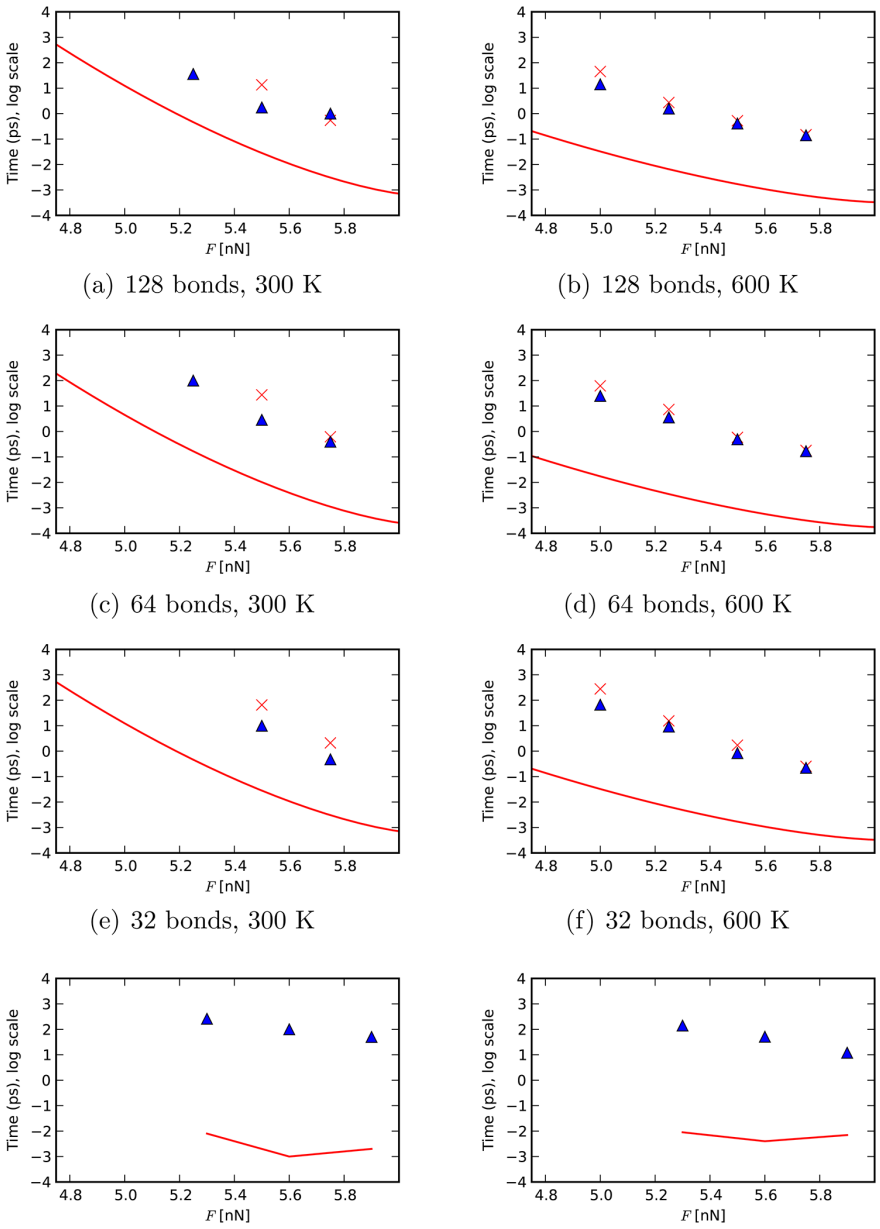

Figure 3. Bond-breaking time as a function of force: − TST, × MD classic sampling, Δ MD quasiclassical sampling. Butane and octane obtained from BOMD, while all others cases are a linear chain of Morse potentials.

higher effciency, the electronic degrees of freedom were propagated using the time-reversible technique of Niklasson et al.[33] Fixed-force sampling was performed with a Python script using the analytical molecular Hessian calculated with DALTON 2011,[32,34] while sudden-force sampling was made with the Gaussian 09 package.[35]

For each molecule and each force (F^{sub},F^{crit}, and F^{super}), we located a transition state on the force-modified PES for a single terminal C−C bond breaking using the trust-radius image method.[36] We have not searched for transition states for multiple bond ruptures as their barriers should be significantly higher than those for single bond ruptures and therefore not affect the TST kinetics.

RESULTS

Fixed-Force Rupture Time. In Figure 3, we have plotted the time to bond rupture against the fixed force, for different systems and temperatures, as calculated using BOMD dynamics (both LCM and DFT) and TST theory.

As seen from Figure 3, TST in all cases predicts a shorter bond-breaking time than does LCM and DFT dynamics; moreover, the bond-breaking time decreases with increasing force in an approximately exponential fashion. For all molecules

dx.doi.org/10.1021/jp504959z | J. Phys. Chem. A 2014, 118, 7683−7694

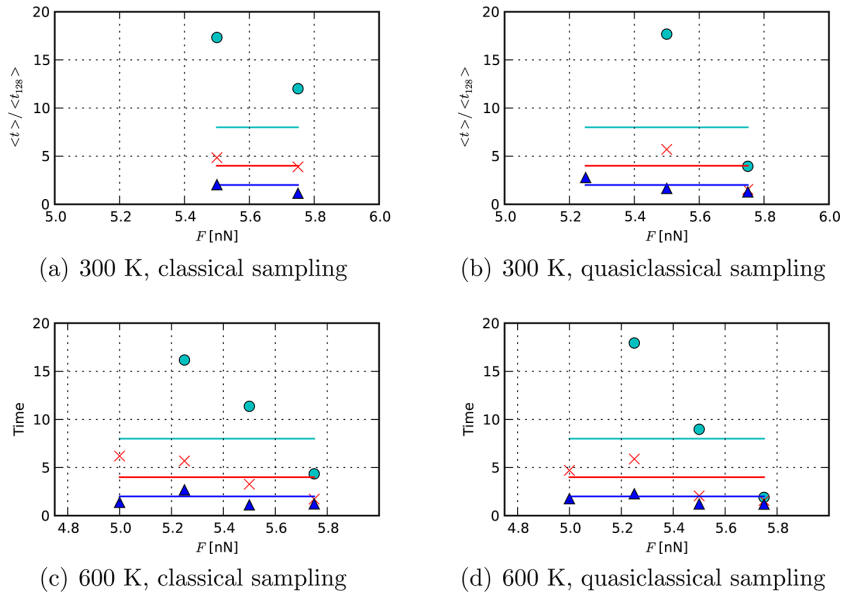

Figure 4. Average bond-breaking time $\langle t_N \rangle$ for a chain of length N relative to $\langle t_{128} \rangle$ as a function of the external force, F. The following color codes apply: $N = 16$ ○ (cyan), $N = 32$ × (red), and $N = 64$ Δ (blue). The solid lines indicate the corresponding factors that result from treating bond breaking as N independent processes, as predicted by eq 16, using the same color codes.

(most strongly for the smallest), TST estimates appear unphysical in the sense that dissociation is predicted to occur at a time down to less than a half period of molecular vibration. In particular, for F^{sub} and F^{crit}, butane and octane are predicted to dissociate instantaneously (in about 1 fs) due to the low barrier, which essentially becomes zero with the inclusion of zero-point vibrational energy corrections. We observe that, for sufficiently large forces, the TST time to rupture becomes equal to the time it takes to stretch the bond by 2 Å. This time is inversely proportional to the square root of the force, yielding the shape observed in the plots. Furthermore, the bond-breaking time becomes considerably shorter at higher temperatures (600 K vs 300 K).

The LCM and DFT dynamics simulations appear to be more realistic than TST, predicting bond-breaking times that are several orders of magnitude longer. The reason for this lies in the statistical hypothesis inherent in TST assuming instantaneous randomization of the energy, while the dynamics simulations incorporate an induction period by allowing sufficient time for energy redistribution, leading to a situation where bond breaking may occur. In other words, the detailed vibrational pattern is important, as discussed in the following.

In the highest-frequency normal mode of the LCM potentials, neighboring bonds vibrate with opposite phases. As a result, the instantaneous energy of a given bond may be greater than the bond dissociation energy (the only requirement for dissociation in TST) but still not break the bond since the actual force on the bond is lower than the external force. On the other hand, the lowest-frequency mode of a linear chain of harmonic oscillators is the totally symmetric vibrational mode, with all atoms moving with the same phase. In this mode, the external force is most effective by elongating all bonds in phase, thereby increasing the likelihood of bond dissociation. For the second lowest-frequency vibrational mode, at the double frequency, all atoms to the left of the center of the chain move in phase, while those to the right move coherently in the opposite phase. This mode will also be effective in accommodating the external force for bond dissociation. In short, bond breaking occurs efficiently only at the time scale of the lower-frequency stretching modes of the molecule. This analysis only holds strictly for nonstretched molecules. Close to and beyond the breaking point, the vibrational characteristics and frequencies change considerably.

If the probability of breaking a given bond is independent of the other bonds present in the system, as assumed in eq 16 (correct for very large molecules), then rupture time should be inversely proportional to the number of bonds in the chain. In Figure 4, we have plotted the average bond-breaking times from the LCM simulations. For easy comparison, the results have been plotted on a relative scale, normalized to the bond-breaking time of the longest chain, with $N = 128$. The solid horizontal lines symbolize the values predicted from eq 16. Whereas, for $N = 64$, the inverse proportionality is well accounted for (a factor of 2), there are marked deviations for the shortest chains: in particular, at low forces.

The plots in Figure 4 also reveal a dependence on the sampling scheme. Not surprisingly, quasiclassical sampling gives shorter bond-breaking times than does classical sampling, mainly because the latter does not include zero-point energy corrections. The small difference between quasiclassical and classical sampling becomes almost insignificant for larger forces and shorter bond-breaking times.

Fixed-Force Bond-Breaking Mechanisms. In the LCM model, all bonds are treated equally. Consequently, the LCM trajectory simulations show that the likelihood for bond dissociation is the same for all bonds along the chain. However, DFT provides a more realistic description of the molecular and electronic structure, predicting a nonuniform probability dissociation along the chain. In addition to the plots in Figures 3g and 3h, the results of the fixed-force DFT calculations are summarized in Table 3, indicating which bond(s) of butane and octane are observed to break. For these small molecules, either

Table 3. Number of Fixed-Force Trajectories for Butane and Octane Leading to: One Bond (Dissociation of One C−C Terminal Bond), Two Bonds (Dissociation of Both Terminal C−C Bonds), sim. (Simultaneous Dissociation of Both Terminal C−C Bonds), and Intact (No Bond Dissociation)[a]

	butane			octane		
force	one bond	two bonds (sim.)	intact	one bond	two bonds (sim.)	intact
F^{sub}	30	17 (2)	1	43	4 (1)	0
F^{crit}	26	21 (3)	0	36	13 (1)	0
F^{super}	4	41 (5)	0	0	35 (15)	0

[a]For octane under F^{sub}, two trajectories result in the breaking of one terminal bond, while one leads to breaking bond number 3.

one or both terminal bonds may break, the latter occurring either simultaneously or consecutively, see Figure 5. The consecutive mechanism dominates: as soon as the first bond is broken, the external force pulls the two fragments apart, thereby generating a traveling shock wave in the larger fragment, which often induces a second bond rupture shortly afterward (see further discussion below).

For F^{sub}, only 2 of 50 trajectories for octane resulted in the breaking of an inner C−C bond. The preference for terminal rather than inner bond breaking (in spite of the inner alkane bonds being thermochemically weaker) has previously been inferred from a static stretching model.[13] We note that, for the weakest force F^{sub}, one butane trajectory did not lead to bond breaking within 2 ps.

The probability that two bonds are broken (either consecutively or simultaneously) increases with increasing force. Thus, for octane, more than half of the trajectories break only one bond with F^{sub} and F^{crit}, while all trajectories break two bonds with the stronger force F^{super}. A similar behavior is observed for butane although some F^{super} trajectories still break only one bond.

When two terminal bonds are broken, we have calculated the average time between the bond ruptures, see Table 4. For butane, the delay time decreases abruptly from F^{sub} to F^{crit} and F^{super}, the latter forces giving almost identical delay times. For octane, the picture is similar but the decrease is less abrupt from F^{sub} to F^{crit} and further to F^{super}.

Table 4. Average Times between Bond Ruptures (fs)

	butane	octane
F^{sub}	93	158
F^{crit}	24	66
F^{super}	23	12

In Figure 6, the delay time divided by the separation between the ruptured bonds is plotted for the supercritical force (for which double rupture is most frequent). For butane, the distribution is centered around 10 km/s, which corresponds to the speed of the shock wave (similar to the speed of sound in light solids). For octane, no peak is observed, suggesting that the shock-wave mechanism is unimportant for this molecule at a high force. The same holds for the LCM simulations with N = 128 (Figure 6c). Also for the LCM model, a shock wave is created after the first bond rupture, but this effect is most clearly observed below F^{crit}, see Figure 6a. This is because at 5.75 nN the probability of breaking the second bond is so large that it becomes the dominant mechanism, giving the shock wave insufficient time to propagate to the other terminus before the second bond breaks. However, we should be careful not to overinterpret our data, bearing in mind that the LCM and DFT models both give a crude description of the anchoring of the end atoms to the source of the external force, which limits the description of how the shock wave is reflected at the termini.

Sudden-Force Rupture Times. The time scale of oscillation of a polymer is correlated with its lowest-frequency vibration, which corresponds to the full period of oscillation of the end atoms. The bond-breaking times on this scale are displayed in Figure 7 for the sudden-force cases investigated.

Applying the force suddenly to the end atoms rather than first allowing the molecule to relax—as described in the two preceding sections—has important implications for the time evolution of the systems. We observe that an external sudden force of only 3.5 nN is sufficient to generate numerous bond ruptures within a 9 ps time frame. This force is significantly smaller than the critical force and also less than that predicted by TST and observed in the fixed-force cases.

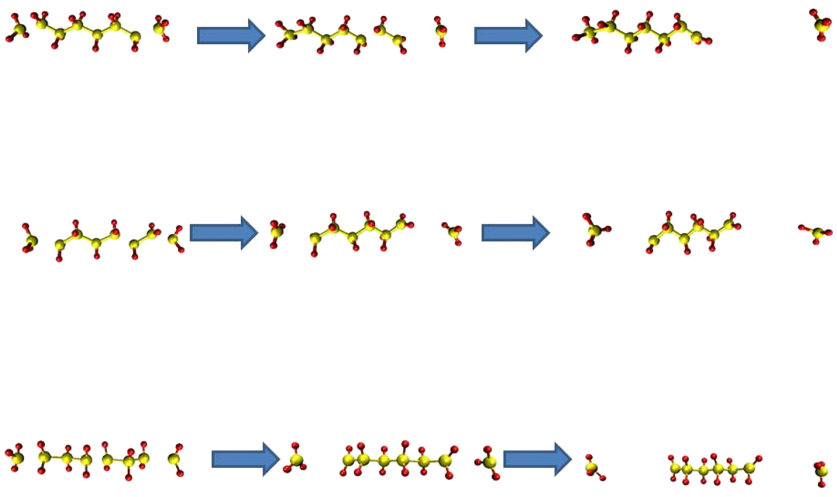

Figure 5. Bond-breaking mechanisms: (top) single bond breaking, (middle) breaking of both terminal bonds with delay, (bottom) simultaneous breaking of both terminal bonds.

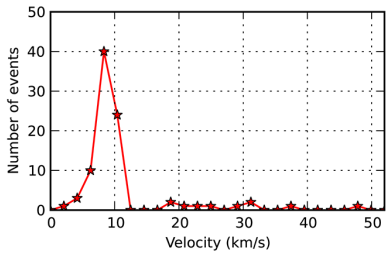

(a) 128 bonds, Classic sampling, 5.25 nN, 600 K

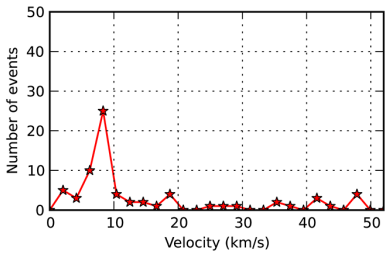

(b) 128 bonds, quasiclassical sampling, 5.75 nN, 300 K

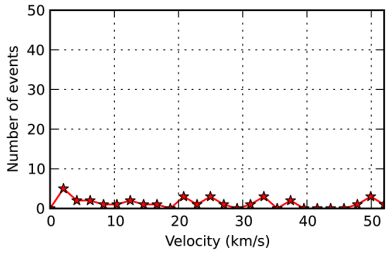

(c) 128 bonds, quasiclassical sampling, 5.75 nN, 600 K

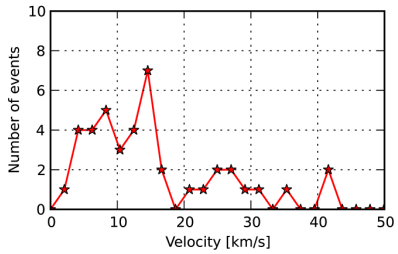

(d) butane, F^{super}, 300 K

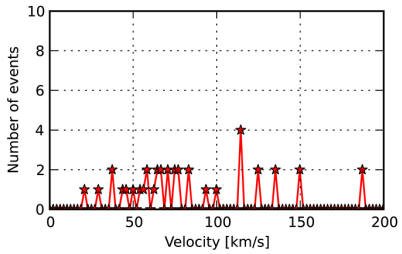

(e) octane, F^{super}, 300 K

Figure 6. Distribution of time between the first and second bond breakage divided by distance between the two bonds broken. The peaks at 10 km/s and 15 km/s represent the speed of a shock wave.

The pulse generated by a sudden application of a force at the termini propagates through the molecule by successively pulling the atoms outward, eventually stretching the central bond. If the molecule has not dissociated at this point, the motion will reverse, propagating from the innermost atoms to the end atoms. At this point, the pulse again reverses, beginning a second vibrational cycle. Since the motion shares the broad features of the lowest vibrational mode, neighboring bonds will typically oscillate in phase, the external forces on a bond ($F_{i-1,i}$ and $F_{i+1,i+2}$) oscillating in phase with the given bond (between atoms i and $i + 1$). This mechanism reduces the energy required to break a bond, causing the opposite effect of the antiphase oscillations that dominate the fixed-force behavior.

The external sudden force F^{ext} (here taken to be 3.5 nN) increases the energy in a single mode of vibration, which may be written as

$$E = \frac{1}{2}mv^2 + \frac{1}{2}k_e x^2 - F^{ext}x \tag{22}$$

If the initial kinetic energy is zero, then this bond will oscillate from $x = 0$ to $x = x_{max}$ where

$$\frac{1}{2}k_e x_{max} = F^{ext} \tag{23}$$

At this point, we can define a corresponding internal force equal to

$$F^{int}(x_{max}) = -k_e x_{max} = -2F^{ext} \tag{24}$$

At maximum elongation, the internal force is twice the external force, that is, 7.0 nN, sufficient for bond breaking. However, some proportion of the introduced energy dissipates into other modes, and we should also include the effects of random thermal motion. The result in eq 24 is therefore only approximate and F^{ext} = 3.5 nN will not necessarily break the chain during the first oscillation period.

From these considerations, we can better understand the results in Figure 7. We also note that the period of vibration of the entire molecule is proportional to the size of the system: the larger the system, the slower the slowest normal mode. However, from Figure 3, it is clear that the larger the molecule (and thus also the slower the vibration), the larger the probability for a bond to break during the first period. For 128 bonds and quasiclassical sampling, all bonds are broken within the first cycle. For 32 bonds, each cycle is faster but the

dx.doi.org/10.1021/jp504959z | J. Phys. Chem. A 2014, 118, 7683−7694

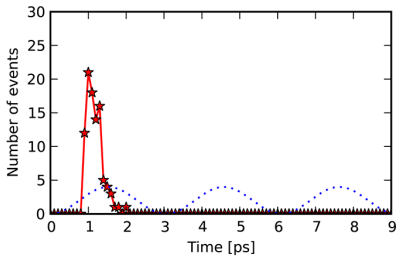

(a) 128 bonds, quasiclassical sampling, 3.5 nN

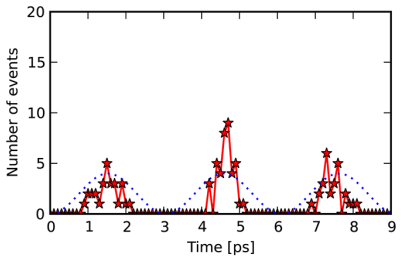

(b) 128 bonds, classical sampling, 3.5 nN

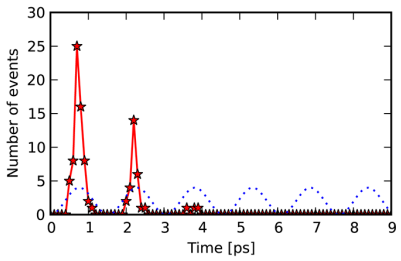

(c) 64 bonds, quasiclassical sampling, 3.5 nN

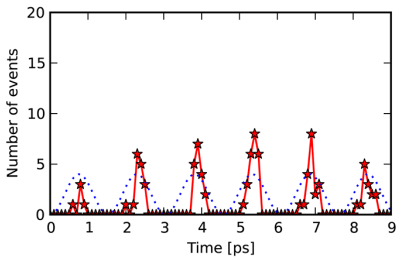

(d) 64 bonds, classical sampling, 3.5 nN

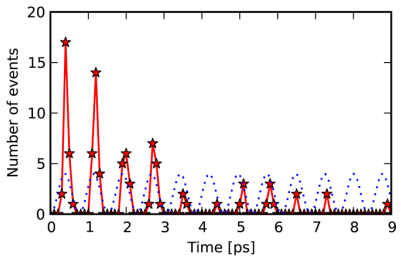

(e) 32 bonds, quasiclassical sampling, 3.5 nN

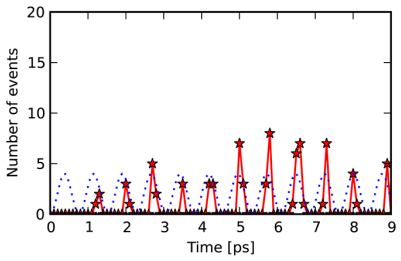

(f) 32 bonds, classical sampling, 3.5 nN

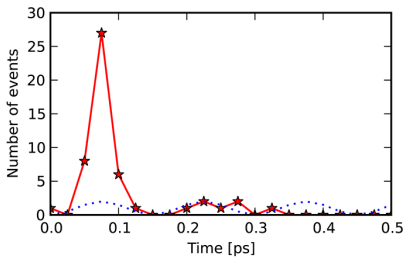

(g) butane, 4.5 nN

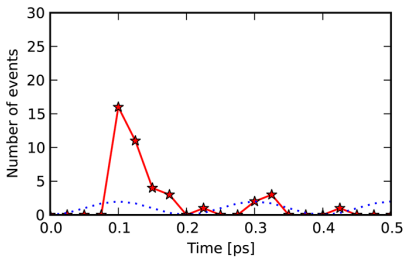

(h) octane, 4.1 nN

Figure 7. Bond-breaking time distribution for different examples (sudden force). The dotted line is the vibration of the elongation for the entire system.

probability of breaking within the first cycle is decreased; for 16 bonds, the bond-breaking probability is distributed all over the time scale.

It is also seen that classical sampling decreases the probability for bond dissociation to occur within the first cycle: the difference between the different sampling schemes appears to be more important with a sudden force than with a fixed force. As a molecule is stretched, its normal-mode frequencies are modified, changing the energetics of the different modes. Stretching induces energy transfer between the different modes of vibration. It is therefore reasonable that a quasiclassical sampling scheme is important when the stretching process is included in the dynamics.

As expected from the considerations above, Figure 7 shows that the bond-breaking time is not randomly distributed in all cases, but follows a cyclic pattern, deviating from a truly exponential decay. A first peak appears when the molecule has reached maximum elongation, according to eq 24. Further peaks occur every time the molecule reaches a similar geometric

dx.doi.org/10.1021/jp504959z | J. Phys. Chem. A 2014, 118, 7683−7694

configuration, the peaks being separated by one vibrational period.

The DFT simulations show a pattern similar to that of the LCM simulations, displaying both a clear correlation between chain length and bond-breaking time and cyclic patterns, see Figure 7. Indeed, most bonds are broken upon maximum elongation during the first cycle. Thus, the importance of the slow stretching modes in the dissociation dynamics revealed for LCM is reaffirmed by the DFT calculations.

Sudden-Force Bond-Breaking Mechanisms. In the fixed-force LCM model calculations, the bond-breaking point is uniformly distributed along the entire length of the chain, in accordance with the fact that all bonds are described by the same Morse parameters. However, this is no longer the case when the force is applied suddenly, see Table 5. Bond breaking occurs only in the central part of the molecule.

Table 5. Position of Bond Breaking for LCM, 128 Bonds, Sudden Force[a]

	1	2	3	4	5	6	7	8	intact
classical sampling	0	0	4	38	44	10	0	0	0
quasiclassical sampling	0	0	2	48	36	9	1	0	0

[a]The molecule has been divided into 8 parts each consisting of 16 bonds, where parts 1 and 8 are the outermost parts, and parts 4 and 5 the innermost. The number of trajectories giving rise to bond dissociation in a given part of the molecule is given.

The DFT sudden-force simulations of butane and octane display a pattern different from that in the fixed-force simulations, see Table 6. For butane, the consecutive breaking

Table 6. Number of Various Bond-Breaking Events for Octane and Butane from sudden-force DFT simulations: One Bond (Dissociation of One C−C Terminal Bond), Two Bonds (Dissociation of Both Terminal C−C Bonds), Central (Dissociation of the Central C−C Bond), 3 + 5 (Dissociation of Third and Fifth C−C Bonds), 2 + 3 + 5 (Dissociation of Second, Third, and Fifth C−C Bonds), 1 + 2 + 5 (Dissociation of First Two C−C Bonds Starting from the Terminal One and the Fifth One), and Intact (No Bond Dissociation)

force	one bond	two bonds	central	3 + 5	2 + 3 + 5	1 + 2 + 5	intact
butane	10	25(2)	13				0
octane	7	0	21	11	3	1	7

of the two terminal bonds still dominates (25 trajectories), but breaking of the middle bond is now also significant (13 trajectories); only 10 trajectories lead to a single terminal bond cleavage. For octane, central-bond cleavage dominates (21 trajectories), but cleavage of a single terminal bond is also frequent (7 trajectories). Cleavage of both terminal bonds is never observed for octane, approaching the results of the longer chains of the LCM calculations.

Statistical and Nonstatistical Dissociation. If unimolecular dissociation is statistical, the number of molecules left (or number of dissociation events) $N(t)$ must change exponentially with time, that is, according to the first-order kinetic equation. This hypothesis has been tested and is roughly satisfied for most data sets, the deviations being due to incomplete statistics. There are also local deviations due to intramolecular vibrational energy redistribution, as discussed above in terms of stretching vibrational cycles (see Figure 7). The exception from the first-order law is sudden-force LCM calculations with classical sampling. Indeed, from Figures 7b, 7d, 7f, and 7h we can see that $N(t)$ is not strictly exponential. This means that the kinetic law is close to zero-order having a constant rate, independent of the number of molecules. Such kinetics is typical for heterogeneous reactions controlled by diffusion. By analogy, we can formally view the dissociation as a two-stage process: intramolecular vibrational energy redistribution (energy "diffusion") followed by dissociation, the former being rate limiting. This is not an unreasonable explanation, since the molecules sampled classically and subject to the sudden force are far from equilibrium.

DISCUSSION

The results presented above show good qualitative agreement between the simple LCM empirical force-field model and the more realistic DFT molecular model. First, the LCM and DFT dynamics simulations both give significantly lower dissociation rates than does the statistical TST. Second, both force field models agree that dissociation occurs at a considerably lower external force in the sudden-force case than in the fixed-force case. Third, for both LCM and DFT, dissociation times correlate with the slowest stretching vibrations of the chain. Finally, the LCM and DFT dissociation rates are similar. The LCM calculations show that the time it takes to break the chain depends on its length, approaching the expected inverse proportional dependence for large systems.

To be more specific, in the sudden-force case, the DFT and LCM dynamics calculations both show a clear preference for dissociation of the central C−C bonds, in agreement with a simple mechanical model. On the other hand, a fixed-force LCM model shows essentially equal probability for any bond of the polymer to be broken, while DFT nonequivocally predicts terminal C−C bonds to be most easily cleaved. The difference arises since, in the LCM model, all bonds are equivalent, having the same Morse potential parameters. In hydrocarbons, the terminal C−C bonds are thermochemically stronger than the central C−C bonds, in contrast to the observations from the fixed-force DFT simulations. However, thermochemical bond stability and resistance to bond stretching, as studied here, are not the same. The force-modified potential energy surface is highly deformed from that of the stable molecule. Upon slow stretching (near the thermodynamical equilibrium), the terminal bond is gradually weakened as the bond angle between the two outermost C−C bonds increases more than do the inner bond angles, reducing the terminal bond strength but also aligning with the external force.[13,20] Such a subtle effect cannot be reproduced by a simple one-dimensional force-field model.

The sudden-force scenario has relevance for the conditions experienced by polymers in solution subject to ultrasound, where sudden deviations far from thermodynamical equilibrium occur. Our dynamical calculations predict cleavage of the central bonds, which needs to be substantiated through experiment.

Despite this optimistic conclusion, there are many pitfalls of applying simple models to complicated problems, as in the well-known case of the 50 year old Fermi−Pasta−Ulam−Tsingou problem, where the harmonic oscillator potential of a vibrating string was augmented by a third-order term.[37,38] The numerical solutions of the original problem[37] were initially a

surprise to the authors, as the energy of one initially excited mode was shown to not spread out to all modes in an ergodic fashion. Instead, the energy started leaking into the closest modes, but after some time the energy reverted to the original mode, a finding that eventually led to chaos theory. This tells us that achieving thermodynamical equilibrium in a vibrating chain is not a trivial problem: in particular, since the role of nonstretching modes has not been studied here. Typical wave phenomena such as standing waves may also be important.

Regardless of these problems, we have shown that it is important to consider the dynamical fluctuations of the forces acting on the atoms of a molecule and their pattern of oscillation. This may be important not only during covalent bond cleavage but also in force-induced chemical reactions. For such reactions, the reaction rate increases under the influence of an external force due to a shift in the relative energies of the transition state and the reactant state. It is not difficult to imagine that the details of how the force is applied may be important for the activation process. For example, it has been demonstrated that ring-opening reactions are activated by the application of ultrasound.[16,19−21,39−41]

CONCLUSION

We have shown that a linear chain of Morse potentials is an appropriate model for studying the fundamental effect of dynamics in the mechanochemistry of polymers, being in good qualitative agreement with the more accurate quantum-chemical calculations of molecules. Provided that Morse potential parameters are properly selected, the agreement is semiquantitative.

The time it takes to break a polymer reaches the expected inverse proportionality to the size of the chain for sufficiently large systems, with more than 50 bonds. As the efficiency of quantum-chemical calculations improves, it will become possible to study these effects in detail using accurate quantum-chemical methods for larger and more complex molecules than those considered here.

We have shown that antiphase vibrational patterns of neighboring bonds significantly improve the mechanochemical strength of a bond at short time scales. In contrast, supplying energy to the lowest stretching mode reduces drastically the external force needed to break a bond. In this manner, neighboring bonds are set to oscillate in phase, enhancing the probability for bond breaking. We have analyzed two extreme scenarious, fixed force and sudden force, to show that dynamics is important to consider when trying to understand experiments in mechanochemistry.

AUTHOR INFORMATION

Corresponding Author

*E-mail: einar.uggerud@kjemi.uio.no. Phone: +47 22855537. Fax: +47 22855441.

Notes

The authors declare no competing financial interest.

ACKNOWLEDGMENTS

The research in Karlsruhe was supported by the Deutsche Forschungsgemeinschaft through the Center for Functional Nanostructures (CFN, Grant No. C3.3). This work was supported by the Norwegian Research Council by the Grant No. 179568/V30, to the Centre of Theoretical and Computational Chemistry through their Centre of Excellence program; and the Norwegian Supercomputing Program (NOTUR) through a grant of computer time (Grant No. NN4654K).

REFERENCES

(1) Beyer, M. K.; Clausen-Schaumann, H. Mechanochemistry: The Mechanical Activation of Covalent Bonds. *Chem. Rev.* **2005**, *105*, 2921−2948.
(2) Kean, Z. S.; Craig, S. L. Mechanochemical Remodeling of Synthetic Polymers. *Polymer* **2012**, *53*, 1035−1048.
(3) Hickenboth, C. R.; Moore, J. S.; White, S. R.; Sottos, N. R.; Baudry, J.; Wilson, S. R. Biasing Reaction Pathways with Mechanical Force. *Nature* **2007**, *446*, 423−427.
(4) Ribas-Arino, J.; Marx, D. Covalent Mechanochemistry: Theoretical Concepts and Computational Tools with Applications to Molecular Nanomechanics. *Chem. Rev.* **2012**, *112*, 5412−5487.
(5) Caruso, M. M.; Davis, D. A.; Shen, Q.; Qdom, S. A.; Sottos, N. R.; Moore, S. R. J. Mechanically-Induced Chemical Changes in Polymeric Materials. *Chem. Rev.* **2009**, *109*, 5755−5798.
(6) Grandbois, M.; Beyer, M.; Rief, M.; Clausen-Schaumann, H. How Strong Is a Covalent Bond? *Science* **1999**, *283*, 1727−1730.
(7) Aniavarapu, S. R. K.; Witta, A. P.; Dougan, L.; Uggerud, E.; Fernandez, J. M. Single-Molecule Force Spectroscopy Measurements of Bond Elongation during a Bimolecular Reaction. *J. Am. Chem. Soc.* **2008**, *130*, 6479−6487.
(8) Kucharski, T. J.; Boulatov, R. The Physical Chemistry of Mechanoresponsive Polymers. *J. Mater. Chem.* **2011**, *21*, 8237−8255.
(9) Ribas-Arino, J.; Shiga, M.; Marx, D. Understanding Covalent Mechanochemistry. *Angew. Chem., Int. Ed.* **2009**, *48*, 4190−4193.
(10) Bell, G. Models for the Specific Adhesion of Cells to Cells. *Science* **1978**, *200*, 618−627.
(11) Kucharski, T. J.; Yang, Q.-Z.; Tian, Y.; Boulatov, R. Strain-Dependent Acceleration of a Paradigmatic S_N2 Reaction Accurately Predicted by the Force Formalism. *J. Phys. Chem. Lett.* **2010**, *1*, 2820−2825.
(12) Iozzi, M. F.; Helgaker, T.; Uggerud, E. Influence of External Force on Properties and Reactivity of Disulfide Bonds. *J. Phys. Chem. A* **2011**, *115*, 2308−2315.
(13) Smalø, H. S.; Uggerud, E. Breaking Covalent Bonds Using Mechanical Force, which Bond Breaks? *Mol. Phys.* **2013**, *111*, 1563−1573.
(14) Lourderaj, U.; McAfee, J. L.; Hase, W. L. Potential Energy Surface and Unimolecular Dynamics of Stretched *n*-Butane. *J. Chem. Phys.* **2008**, *129*, 094701-1−094701-10.
(15) Saitta, A. M.; Klein, M. L. Polyethylene Under Tensile Load: Strain Energy Storage and Breaking of Linear and Knotted Alkanes Probed by First-principles Molecular Dynamics Calculations. *J. Chem. Phys.* **1999**, *111*, 9434−9440.
(16) Ribas-Arino, J.; Shiga, M.; Marx, D. Mechanochemical Transduction of Externally Applied Forces to Mechanophores. *J. Am. Chem. Soc.* **2010**, *132*, 10609−10614.
(17) Konda, S. S. M.; Brantley, J. N.; Bielawski, C. W. Chemical Reactions Modulated by Mechanical Stress: Extended Bell Theory. *J. Chem. Phys.* **2011**, *135*, 164103-1−164103-8.
(18) Mason, T. Ultrasound in Synthetic Organic Chemistry. *J. Chem. Soc. Rev.* **1997**, *26*, 443−451.
(19) Brantley, J. N.; Wiggins, K. M.; Bielawski, C. W. Unclicking the Click: Mechanically Facilitated 1,3-Dipolar Cycloreversions. *Science* **2011**, *333*, 1606−1609.
(20) Smalø, H. S.; Uggerud, E. Ring Opening vs. Direct Bond Scission of the Chain in Polymeric Triazoles under the Influence of an External Force. *Chem. Commun.* **2012**, *48*, 10443−10445.
(21) Ong, M. T.; Leiding, J.; Tau, H.; Virshup, A. M.; Martinez, T. J. First Principles Dynamics and Minimum Energy Pathways for Mechanochemical Ring Opening of Cyclobutene. *J. Am. Chem. Soc.* **2009**, *131*, 6377−6379.
(22) Lenhardt, J. M.; Ong, M. T.; Choe, R.; Evenhuis, C. R.; Martinez, T. J.; Craig, S. L. Trapping a Diradical Transition State by Mechanochemical Polymer Extension. *Science* **2010**, *329*, 1057−1060.

(23) Hofbauer, F.; Frank, I. CPMD Simulation of a Bimolecular Chemical Reaction: Nucleophilic Attack of a Disulfide Bond under Mechanical Stress. *Chem.—Eur. J.* **2012**, *18*, 16332−16338.
(24) Dopieralski, P.; Ribas-Arino, J.; Anjukandi, P.; Krupicka, M.; Kiss, J.; Marx, D. The Janus-faced Role of External Forces in Mechanochemical Disulfide Bond Cleavage. *Nat. Chem.* **2013**, *5*, 685−691.
(25) Iozzi, M. F.; Helgaker, T.; Uggerud, E. Assessment of Theoretical Methods for the Determination of the Mechanochemical Strength of Covalent Bonds. *Mol. Phys.* **2009**, *107*, 2537−2546.
(26) Wolinski, K.; Baker, J. Geometry Optimization in the Presence of External Forces: a Theoretical Model for Enforced Structural Changes in Molecules. *Mol. Phys.* **2010**, *108*, 1845−1856.
(27) Florencio, J., Jr.; Lee, M. H. Exact Time Evolution of a Classical Harmonic-oscillator Chain. *Phys. Rev. A* **1985**, *31*, 3231−3236.
(28) Hase, W. L.; Buckowski, D. G. Monte Carlo Sampling of a Microcanonical Ensemble of Classical Harmonic Oscillators. *Chem. Phys. Lett.* **1980**, *74*, 284−287.
(29) Lu, D.-H.; Zhao, M.; Truhlar, D. G. Projection Operator Method for Geometry Optimization with Constraints. *J. Comput. Chem.* **1991**, *12*, 376−384.
(30) Verlet, L. Computer "Experiments" on Classical Fluids. I. Thermodynamical Properties of Lennard-Jones Molecules. *Phys. Rev.* **1967**, *159*, 98−103.
(31) LSDALTON, a Linear Scaling Molecular Electronic Structure Program, Release Dalton 2011 (2011), see http://daltonprogram.org/.
(32) Aidas, K.; Angeli, C.; Bak, K. L.; Bakken, V.; Bast, R.; Boman, L.; Christiansen, O.; Cimiraglia, R.; Coriani, S.; Dahle, P.; et al. The Dalton Quantum Chemistry Program System. *Wiley Interdiscip. Rev.: Comput. Mol. Sci.* **2014**, *4*, 269−284.
(33) Niklasson, A.; Tymczak, C.; Challacombe, M. Time-Reversible Born-Oppenheimer Molecular Dynamics. *Phys. Rev. Lett.* **2006**, *97*, 123001-1−123001-4.
(34) DALTON, a Molecular Electronic Structure Program, Release Dalton 2011 (2011), see http://daltonprogram.org/.
(35) Frisch, M. J.; Trucks, G. W.; Schlegel, H. B.; Scuseria, G. E.; Robb, M. A.; Cheeseman, J. R.; Scalmani, G.; Barone, V.; Mennucci, B.; Petersson, G. A.; et al. *Gaussian 09, Revision D.01*; Gaussian, Inc.: Wallingford, CT, 2009.
(36) Helgaker, T. Transition-state Optimizations by Trust-region Image Minimization. *Chem. Phys. Lett.* **1991**, *182*, 503−510.
(37) Fermi, E.; Pasta, J.; Ulam, S. Studies of Nonlinear Problems; *Los Alamos preprint LA-1940*, **1955**. Ford, J. The Fermi-Pasta-Ulam Problem: Paradox Turns Discovery. *Phys. Rep.* **1992**, *213*, 271−310.
(38) Berman, G. P.; Izrailev, F. M. The Fermi-Pasta-Ulam problem: Fifty Years of Progress. *Chaos* **2005**, *15*, 015104-1−015104-18.
(39) Yang, Q.-Z.; Haung, Z.; Kucharski, T. J.; Khvostichenko, D.; Chen, J.; Boulatov, R. A Molecular Force Probe. *Nat. Nanotechnol.* **2009**, *4*, 302−306.
(40) Akbulatov, S.; Tian, Y.; Boulatov, R. Force−Reactivity Property of a Single Monomer Is Sufficient To Predict the Micromechanical Behavior of Its Polymer. *J. Am. Chem. Soc.* **2012**, *134*, 7620−7623.
(41) Brantley, J. N.; Konda, S. S. M.; Makarov, D. E.; Bielawski, C. W. Regiochemical Effects on Molecular Stability: A Mechanochemical Evaluation of 1,4- and 1,5-Disubstituted Triazoles. *J. Am. Chem. Soc.* **2012**, *134*, 9882−9885.